Scientific Research Publishing

Modern Mechanical Engineering, 2022, 12, 45-61
https://www.scirp.org/journal/mme
ISSN Online: 2164-0181
ISSN Print: 2164-0165

Numerical Study of Mixed Convection in an Isosceles Trapezoidal Cavity with Several Outlets: Application for Primary Air Draft in ASUTO Charcoal Stove

Gagnon Koffi Apedanou[1], Kokou N'wuitcha[2], Yendoubé Lare[1], Kossi Napo[1]

[1]Laboratoire sur l'Energie Solaire, Chair Unesco, Faculté des Sciences, Université de Lomé, Lomé, Togo
[2]Laboratoire sur l'Energie Solaire, Groupe Phénomènes de Transfert et Energétique (LES-GPTE), Faculté des Sciences, Université de Lomé, Lomé, Togo
Email: gagnonjoseph@yahoo.fr

How to cite this paper: Apedanou, G.K., N'wuitcha, K., Lare, Y. and Napo, K. (2022) Numerical Study of Mixed Convection in an Isosceles Trapezoidal Cavity with Several Outlets: Application for Primary Air Draft in ASUTO Charcoal Stove. *Modern Mechanical Engineering*, **12**, 45-61.
https://doi.org/10.4236/mme.2022.122003

Received: January 9, 2022
Accepted: May 20, 2022
Published: May 23, 2022

Abstract

Mixed convection of heat and mass transfer in an isosceles trapezoidal cavity has been studied numerically. Constant heat flux is imposed through four outlets and the grid is insulated. The inclined walls are maintained in natural convection while the lower horizontal wall is adiabatic. These conditions reflect the air draft zone of the ASUTO charcoal stove. The governing two-dimensional flow equations have been solved by using the finite difference method and Thomas's algorithm. The investigations are conducted for different values of Richardson (R_i), Reynolds number (R_e) and inclination angles of sidewalls. The results are presented in terms of streamlines, isotherms, moisture contours. It was found that for Reynolds number (R_e) equal to 100, the flow pattern is strongly dependent on the inclination angle and Richardson number. Thus, for high Richardson number (R_i) values (10, 100), the dominance of natural convection over the flow structure decreases with the decreasing of the inclination angle of sidewalls of the cavity. For $R_i = 1$, an optimum air draft corresponds to an inclination angle in the vicinity of 22˚ while for $R_i =$ 10 or 100 (in dominance of natural convection), the optimum inclination angle for air draft is in the vicinity of 15˚.

Keywords

Mixed Convection, Heat and Mass Transfer, Trapezoidal Cavity, ASUTO Charcoal Stove, Richardson Number, Several Outlets

1. Introduction

The phenomenon of thermal convection has been the subject of numerous research activities. On the one hand, energy efficiency in industrial or semi-industrial processes has prompted a great number of authors to take interest in the subject. On the other hand, it has been shown that the efficiency of combustion processes in improved stoves depended primarily on their air draft [1]. Dr. Larry Winiasky [2] in the "design principles for wood burning cookstoves", proposes ten design principles for an efficient biomass cookstove with low emission rates. In these ten principles, five of them refer to an optimal draught of air in the cookstove. An insufficient amount of air in the combustion chamber leads to incomplete combustion with a high emission rate and little heat. Too much air flow also prevents the combustion gas from burning in the stove: this is sometimes the case with forced draught stoves. According to Kumar *et al.* [3], in a natural draught stove, the best mixing of fuel gases could not take place. Therefore, the stove developer has to improve the combustion efficiency by means of better stove geometry and new materials. Combustion in a solid fuel stove is largely dependent on the flow of fluid through the fuel bed. MacCarty *et al.* [4] studied the performance of the Rocket stove and concluded that a well-designed stove with optimal geometry can result in better air distribution in the bed and drafting of flue gases out of the kitchen. According to Baldwin [5]; the performance of the stove can be improved by injecting air below the fuel bed for better air mixing, which is necessary for clean burning of the fuel. This will increase the thermal efficiency and reduce the emissions of the stove. The efficiency of the stove can be increased by controlling the air flow to the combustion chamber. In addition, optimal flow not only improves combustion efficiency and temperature, but also reduces emissions. Agenbroad *et al.* [6], [7] proposed a simplified model of the fundamental physics of the natural draft stove to predict the flow rate, temperature and excess air ratio as a function of stove geometry and firepower. They demonstrated that these parameters are the fundamentals for the work on understanding and improving the emissions and heat transfer of biomass cookstoves. Buoyancy is one of the important input parameters for models of thermal efficiency and heat transfer to the pot; whether the model is analytical, empirical or numerical. On the other hand, excess air rate and oxygen flow rate affect combustion chemistry and aerodynamics, and thus the resulting emissions and heat transfer. Their results point to excess air rate as a promising tool for reducing carbon monoxide emissions. Sedighi and Salarian [1] presented in their literature review a holistic analysis of the parameters which influence the efficiency and the emission rate of stoves. Their analysis shows that the air flow rate in the charcoal cookstove and the heat produced by the charcoal vary in the same way. When the air flow rate increases, the heat produced increases. With respect to the above literature review, we concluded that the study of thermo convection in the geometry of improved stoves would contribute to the optimization of their energy efficiency and their emissions. Concerning the study of convection in cav-

ities, there is a lot of works carried out by researchers. Some authors have studied the phenomenon in simple geometries such as the square cavity [8], the rectangular cavity and other more complex geometries [9] [10] [11] [12], but it should be noted that, to date, few works have focused on the trapezoidal configuration.

From 1989, Lam *et al.* [13] studied experimentally and numerically the natural convection heat transfer in trapezoidal cavity having a hot horizontal base, a cool inclined top and insulated vertical walls. The results are presented for width-to-mean height ratio of 4, Rayleigh numbers from 103 to 107 and top surface inclinations from 0 to 25˚ to the horizontal. Nusselt numbers computed by the model are in good agreement with the experimental values. The results showed higher Nusselt than expected in the range of $8.103 < Ra < 2.105$ for inclinations of 0 to 5˚. The Nusselt number decreases overall, as the inclination increases. The proportions of convective heat flow rate into the high side and low side of the cavity were measured and show distinct maxima at particular Rayleigh numbers independently to the top surface inclination angle. Mohammed Boussaid *et al.* [14] studied the natural transfer of heat and mass in a trapezoidal cavity heated by the base and cooled by the upper inclined wall. The equations relating to the transport of momentum, energy and concentration are solved by the finite volume method. The results showed flow patterns dependent on the inclination of the top wall. Thus, for low angles of inclination, the flow was of the Rayleigh-Bernard type; and for strong inclinations, the flow was more akin to the case of the rectangular cavity heated differentially. The increase in the elongation of the cavity leads to an increase in the rates of heat and mass transfer. Acharya *et al.* [15] investigated the effect of baffles placed on the inclined upper wall of trapezoidal cavity. The results obtained with air as working fluid reveals a decrease in heat transfer in the presence of baffles. In general, the heat transfer decreases when the height of the baffles is increased. Fontana *et al.* [16] studied the effect of two baffles placed at the floor wall of trapezoidal cavity heated differentially on the vertical walls. The results reveal that the presence of the second baffle decreases the cavity's fluid flow and heat transfer. As the height of the second baffle rises, the heat transfer drops drastically. Also, two baffles produce more pronounced thermal stratification than only one. Da Silva *et al.* [17] take up the work done by Fontana *et al.* [16] but go further by proposing a correlation for the average Nusselt number in terms of Prandtl and Rayleigh numbers, the inclination of the upper surface of the cavity and for each baffle height. In addition to the previous results, it was observed that for a given baffle height, the total heat transfer increased substantially with increasing Rayleigh numbers, while the average Nusselt increased smoothly with an increasing tilt angle. Benzema *et al.* [18] present a numerical investigation of steady and laminar mixed convection flow within an irregular ventilated enclosure, crossed by Cu-Water Nano fluid. The bottom wall is maintained at a constant and uniform temperature, whereas the top and the vertical walls are adiabatic. The inclined wall is kept at a lower constant temperature. The governing coupled equations are resolved by the means

of the finite volume technique. The computations are performed using a home-made computer code, which was successfully validated, after comparison of the results with pervious numerical and experimental works. The results are analyzed through dynamic and thermal fields with a particular attention to the Nusselt number evaluated along the active wall. The results reveal that the flow structure is more sensitive to both Richardson and Reynolds numbers variations. Munshi *et al.* [19] studied numerically the mixed convection in a lid-driven hexagonal cavity with corner heater by employing finite element method. The focus of the work is to investigate the effect of Hartmann number, Richardson number, Grashof number and Reynolds number on the fluid flow and heat transfer characteristics inside the enclosure. The results reveal that heat transfer rate increases with increasing Richardson number and Hartmann number. The large values of Richardson number lead to increase the lid-driven effect whereas the small values of Richardson number lead to increase effect of presence of the heat source on the flow and heat characteristics. Thus, heat transfer is enhanced by the increase of Richardson and Reynolds numbers. Benzema *et al.* [20] investigate numerically the effect of an external magnetic field on heat transfer and entropy generation of Ag-MgO/water hybrid nanofluid flow in a partially heated irregular ventilated trapezoidal cavity. A finite volume Fortran code has been written to solve the governing partial differential equations. The analysis has been done for a wide range of Reynolds number, Hartmann number and total nanoparticle volume fraction. The results reveal that the intensification of the magnetic field tends to attenuate the heat transfer convection and to reduce the thickness of the thermal boundary layer, close to the active walls. Globally, adding nanoparticles to the base fluid improves the heat transfer but increases the total entropy generation. This literature review on the study of thermoconvection in trapezoidal cavities shows that most works has been done on the trapezoidal cavity with a single inclined wall. But the case of an isoscele trapezoidal cavity with several outlets has not been studied to date, at least to our knowledge.

In the present study, the case of heat and mass transfer in a trapezoidal cavity representing the primary air draft zone of the ASUTO charcoal stove is presented. The Reynolds is fixed at 100 while the Richardson varies from 0.1 to 100. Thus, the influence of the Richardson and inclination angle of sidewalls on the flow structure, the distribution of temperature and moisture are investigated in detail in order to predict the optimum inclination angle corresponding to the best draft of primary air in ASUTO charcoal stove. This paper is structured as follows: we first present the physical model and simplifying assumptions, then the dimensionless theoretical model with boundary conditions, the numerical methodology used, the results and discussions, and finally a conclusion reporting the main results.

2. Description of the Physical Model

The geometry of the problem under consideration is illustrated in **Figure 1**. This

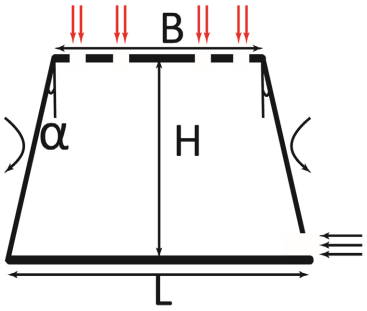

Figure 1. Geometry of the air draft zone of the ASUTO charcoal stove.

is the air draft zone of an improved charcoal stove of isoscele trapezoidal section. The side walls, inclined at an angle α with respect to the vertical, are stationary and maintained in natural convection with the ambient air. An inlet is located on the lower part of right sidewall where primary air enters in the draft zone of ASUTO charcoal stove. The upper horizontal wall is a ceramic grate opening into the combustion zone of the stove. This wall is modeled here by four outlets of the same diameter above which is located a constant heat source q representing the heat flow coming from the charcoal bed of the combustion chamber according to Gogoi and Baruah [21]. The intermediate part of the outlets is kept adiabatic due to its ceramic nature. The lower horizontal wall is assumed adiabatic.

3. Simplifying Assumptions

To carry out the present study, the following simplifying assumptions are considered. Humid air is Newtonian, incompressible and obeys Boussinesq's hypothesis. The physical properties are constant, the Soret and Dufour cross effects are negligible. The regime is laminar and the flow is two-dimensional. Radiant heat transfer is negligible. The viscous dissipation and the pressure term in the heat equation are negligible.

4. Mathematical Model

Taking into account the assumptions made previously, the equations of the mathematical model in dimensionless form are as follows:

$$\frac{\partial U}{\partial X}+\frac{\partial V}{\partial Y}=0 \tag{1}$$

$$\frac{\partial U}{\partial \tau}+U\frac{\partial U}{\partial X}+V\frac{\partial U}{\partial Y}=-\frac{\partial P}{\partial X}+\frac{1}{R_e}\left(\frac{\partial^2 U}{\partial X^2}+\frac{\partial^2 U}{\partial Y^2}\right) \tag{2}$$

$$\frac{\partial V}{\partial \tau}+U\frac{\partial V}{\partial X}+V\frac{\partial V}{\partial Y}=-\frac{\partial P}{\partial Y}+\frac{1}{R_e}\left(\frac{\partial^2 V}{\partial X^2}+\frac{\partial^2 V}{\partial Y^2}\right)+R_i\theta+R_{iC}C \tag{3}$$

$$\frac{\partial \theta}{\partial \tau}+U\frac{\partial \theta}{\partial X}+V\frac{\partial \theta}{\partial Y}=\frac{1}{R_eP_r}\left(\frac{\partial^2 \theta}{\partial X^2}+\frac{\partial^2 \theta}{\partial Y^2}\right) \tag{4}$$

$$\frac{\partial C}{\partial \tau}+U\frac{\partial C}{\partial X}+V\frac{\partial C}{\partial Y}=\frac{1}{S_c}\left(\frac{\partial^2 C}{\partial X^2}+\frac{\partial^2 C}{\partial Y^2}\right) \tag{5}$$

Using the stream function (ψ)-vorticity (ω) formulation, Equations (2) and (3) are reduced in the form:

$$\frac{\partial \omega}{\partial \tau}+U\frac{\partial \omega}{\partial X}+V\frac{\partial \omega}{\partial Y}=\frac{1}{R_e}\left(\frac{\partial^2 \omega}{\partial X^2}+\frac{\partial^2 \omega}{\partial Y^2}\right)+R_i\frac{\partial \theta}{\partial X}+R_{iC}\frac{\partial C}{\partial X} \tag{6}$$

where:

$$\frac{\partial^2 \psi}{\partial X^2}+\frac{\partial^2 \psi}{\partial Y^2}=-\omega \tag{7}$$

$$U=\frac{\partial \psi}{\partial Y} \tag{8}$$

$$V=-\frac{\partial \psi}{\partial X} \tag{9}$$

The dimensional variables are as follows:

$$\begin{gathered} X=\frac{x}{H};\ Y=\frac{y}{H};\ \tau=\frac{tu_0}{H};\ U=\frac{u}{u_0};\ V=\frac{v}{u_0};\ \theta=\frac{T-T_0}{\frac{qh}{\lambda}}; \\ C=\frac{c}{c_0};\ R_e=\frac{u_0 H}{\nu};\ R_i=\frac{Gr}{R_e^2};\ G_r=g\cdot\beta_T\cdot\frac{qH^4}{\nu^2\lambda} \end{gathered} \tag{10}$$

where U and V are the velocity components in X and Y directions respectively, P is the pressure, θ is the non-dimensional temperature, P_r the Prandtl number, S_c the Schmidt number, C the dimensionless concentration, τ the dimensionless time and G_r the Grashof number.

5. Boundary Conditions

5.1. Velocity Components Conditions

All the walls of the cavity have no-slip boundary conditions: on all the walls, the velocities are set to zero:

$$U=V=0 \tag{11}$$

The U component of the velocity is imposed on the inlet while the gradients of the U and V components of the velocity are zero on the outlets.

5.2. Thermal and Moisture Conditions

The experiment study of Biswajit Gogoi and DC Baruah [22] shows that the primary air receives heat from the fuel bed when pulled upward [21]. In order to take into account this experimental observation, a heat flux has been imposed through the outlets. The exits are separated by adiabatic wall.

- Exits

$$\begin{gathered} -\frac{4B}{9H}\le X\le -\frac{3B}{9H};\ \text{or}\ -\frac{2B}{9H}\le X\le -\frac{B}{9H};\ \text{or}\ \frac{B}{9H}\le X\le \frac{2B}{9H}; \\ \text{or}\ \frac{3B}{9H}\le X\le \frac{4B}{9H};\ \text{and}\ Y=1:\frac{\partial \theta}{\partial Y}=1;\frac{\partial C}{\partial Y}=0;\frac{\partial \omega}{\partial Y}=0 \end{gathered} \tag{12}$$

- Walls between exits:

$$-\frac{B}{2H} \le X \le -\frac{4B}{9H};\ \text{or}\ -\frac{3B}{9H} \le X \le -\frac{2B}{9H};\ \text{or}\ -\frac{B}{9H} \le X \le +\frac{B}{9H};$$
$$\text{or}\ \frac{2B}{9H} \le X \le \frac{3B}{9H};\ \text{or}\ \frac{4B}{9H} \le X \le \frac{B}{2H}\ \text{and}\ Y = 1 : \frac{\partial \theta}{\partial Y} = 0; C = 0; \omega = \frac{\partial U}{\partial Y} \quad (13)$$

- On the side walls:

$$-\lambda \frac{\partial \theta}{\partial n} = h\theta; \frac{\partial C}{\partial n} = 0;\ \text{and}\ \omega = \frac{\partial V}{\partial X} - \frac{\partial U}{\partial Y} \quad (14)$$

With n the outgoing normal of the wall.

- Air inlet

$$\theta = 0; C = 1;\ \text{and}\ \omega = \frac{\partial V}{\partial X} - \frac{\partial U}{\partial Y} \quad (15)$$

- On the lower horizontal wall

$$-\frac{L}{2H} \le X \le +\frac{L}{2H}\ \text{and}\ Y = 0 : \frac{\partial \theta}{\partial Y} = 0; \frac{\partial C}{\partial X} = 0; \omega = -\frac{\partial^2 \psi}{\partial Y^2} \quad (16)$$

6. Numerical Method

Transfer equations with boundary conditions are discretized using the implicit finite difference method. The diffusion terms are approximated by the central finite difference scheme while the time derivative is implicitly discretized. The Thomas algorithm was used to solve the algebraic equations system. The simulation is performed numerically using a computer code implemented in Fortran language. The iterative process reaches convergence when the relative variation of the dependent variables (U, V, θ, C or ψ) between actual and the previous iteration is not significant:

$$\left| \frac{f^{n+1} - f^n}{f^{n+1}} \right| \le 10^{-8} \quad (17)$$

where f is the dependent variable, n the previous iteration and $n + 1$, the current iteration.

The transport equations are discretised on a uniformly structured computational domain. The inclined walls are approximated by a staircase shape which, by densifying the mesh, significantly reduces the error generated by this shape. Details of this approach can be found in Mahmoudi *et al.* [22]. The 151 × 101 mesh size was chosen, for a cavity of elongation Al = 1, as providing results very little dependence on the grid except for the case of a 15˚ inclination where 101 × 101 has been retained. The accuracy of the numerical model was verified by comparing results from the present study with those obtained by Aydin *et al.* [23] and Mohammed Boussaid *et al.* [14].

First, we qualitatively compared the flow structure as well as the isotherms obtained by Aydin *et al.* [23], for the case of mixed air convection filling a square cavity with moving walls and heated from below and in the middle. As it can be seen on **Figure 2**, a great similarity is noted between the streamlines and the

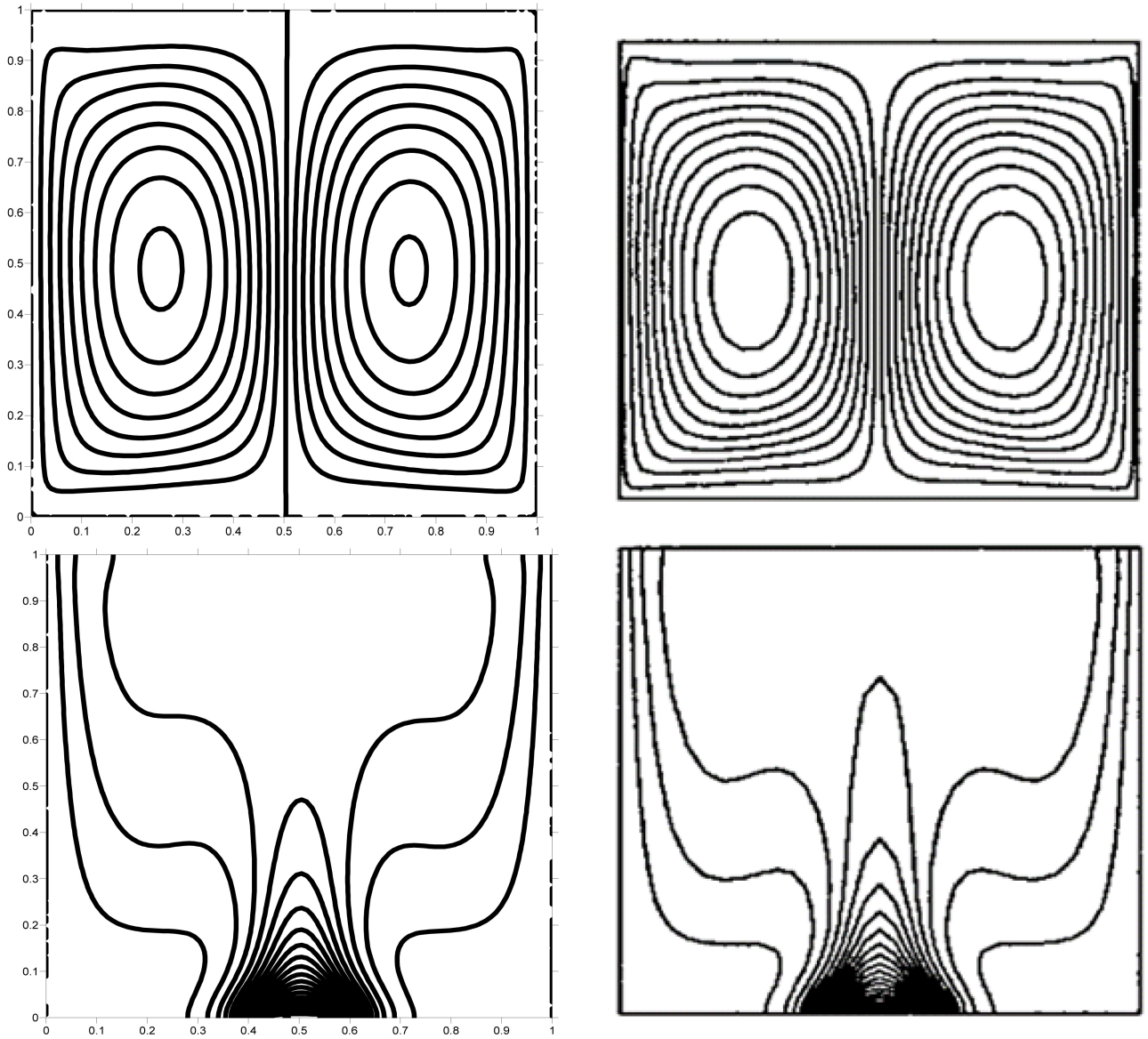

Figure 2. Comparison of streamlines lines and isotherms of the present work (left) with that of Orhan Aydin (right).

isotherms, obtained by the present code and those of Aydin *et al.* [23]. We compared quantitatively on **Figure 3**, the nondimensional vertical velocity profiles at the vertical midplane of the cavity for $R_i = 2$ and for $R_i = 10$.

Secondly, we also qualitatively compared the flow structure as well as the isotherms obtained by Boussaid *et al.* [14], for the case of natural air convection filling a closed trapezoidal cavity heated differentially. As shown on **Figure 4**, one notes a perfect agreement between the steeamlines and the isotherms, obtained by our calculation code and those of the reference Boussaid *et al.* [14].

7. Results and Discussions

Throughout this paper, the Reynolds number and Prandtl number are fixed respectively at R_e = 100 and P_r = 0.71. The effects of physical and geometrical

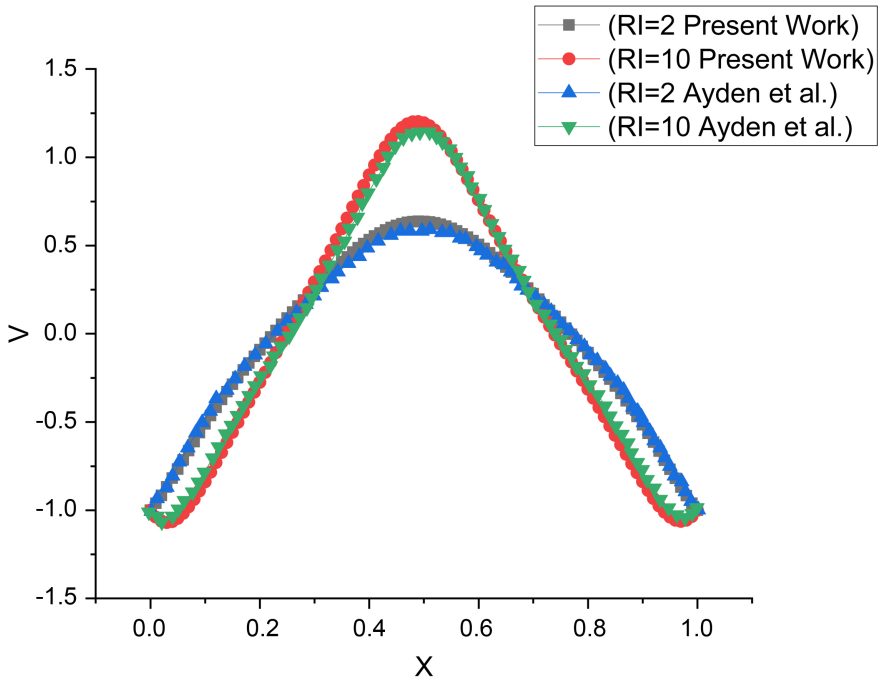

Figure 3. Comparison of the nondimensional vertical velocity profiles at the vertical mid-plane of the cavity for $R_i = 2$ and for $R_i = 10$ (results of Aydin *et al.* and present work).

parameters on the heat transfer and the flow field that occur in the defined cavity are investigated. The analysis has been conducted for the various ranges of non-dimensional parameters such as Richardson number ($0.1 \leq R_i \leq 100$) and the inclination angles ($15^\circ \leq \alpha \leq 30^\circ$) of the sidewalls with respect to the vertical axe. The value of Richardson number determines the dominance of the type of convection. For $Ri < 1$, forced convection is dominant while $R_i > 10$, the free convection is significant. Lastly when $0.1 < R_i < 10$ both convections are significant. This convection is qualified mixed convection.

7.1. Dominance of Forced Convection ($R_i = 0.1$)

The flow structure, the thermal and moisture fields are respectively, presented by the streamlines, isotherms and iso-values of moisture in **Figure 5**, for $R_i = 0.1$ and for the inclination angle varying between 15˚ and 30˚. It can be seen that the streamlines, isotherms and iso-values of moisture patterns are strongly modified by the variation of the inclination angle of sidewalls. The fluid flow is characterized by opened lines spouting from the inlet, along the right inclined wall of the cavity and exits through the closest outlet to this wall on the top grid of the cavity. It appears at the left of the jet of the forced flow observed along the right sidewall of the cavity, a recirculating cell occupying the major part of the cavity (**Figure 5(a)**), when the inclination angle changes from 15˚ to 22˚. The distribution of heat in the cavity conforms to the circulation of the fluid revealed by the streamline's patterns. The isothermal contour patterns are clustered near the top wall and the left sidewall resulting in steep temperature gradient in this zone.

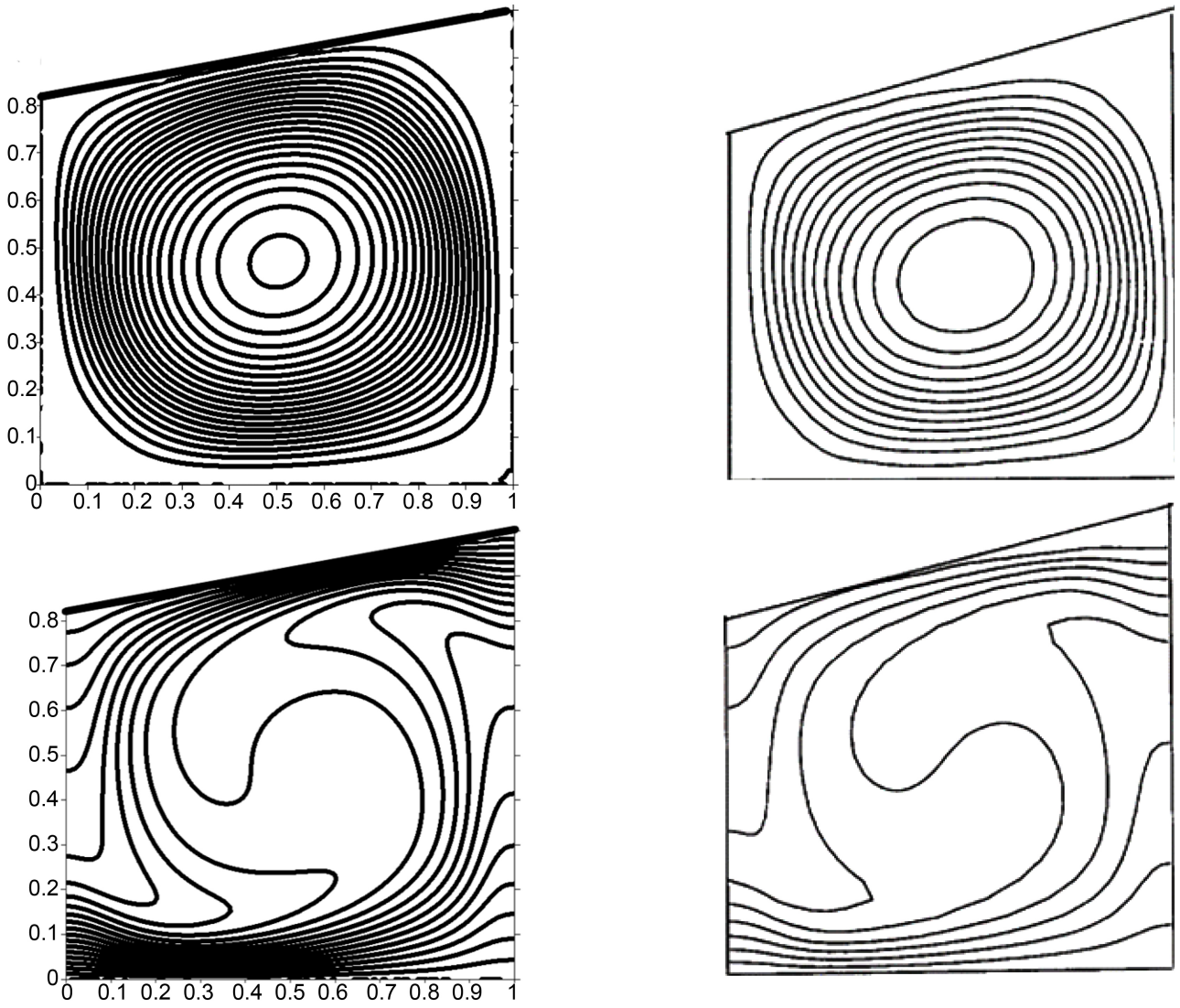

Figure 4. Comparison of streamlines and isotherms of our work (left) with that of Mohammed Boussaid (right).

Indeed, the air moving near the hot grill heats up and by convection, transfers the heat to the rest of the study domain. That is the reason why the values of temperature are higher at the upper part of the cavity. The temperature at the vicinity of the right sidewall where is located the inlet is lower because of the cold jet entering in the cavity. This zone is characterized by the opened lines of streamlines contours dominated by forced flow. Near the left sidewall, it can be noticed parallel isothermal lines denoting the loss of heat by convection trough the left sidewall. By increasing the inclination angle α, the recirculating cell size grows up and turns into opened lines (**Figure 5(a)**) denoting the dominant of forced convection. The contours of moisture (**Figure 5(c)**), show that the moisture is uniform in the zone located between the top grid, the left sidewall and the main flow region where the temperature values are more important. However, it can be observed the clustered contours of moisture in the main flow part. This result reveals the intensification of the diffusion of moisture promoted by the

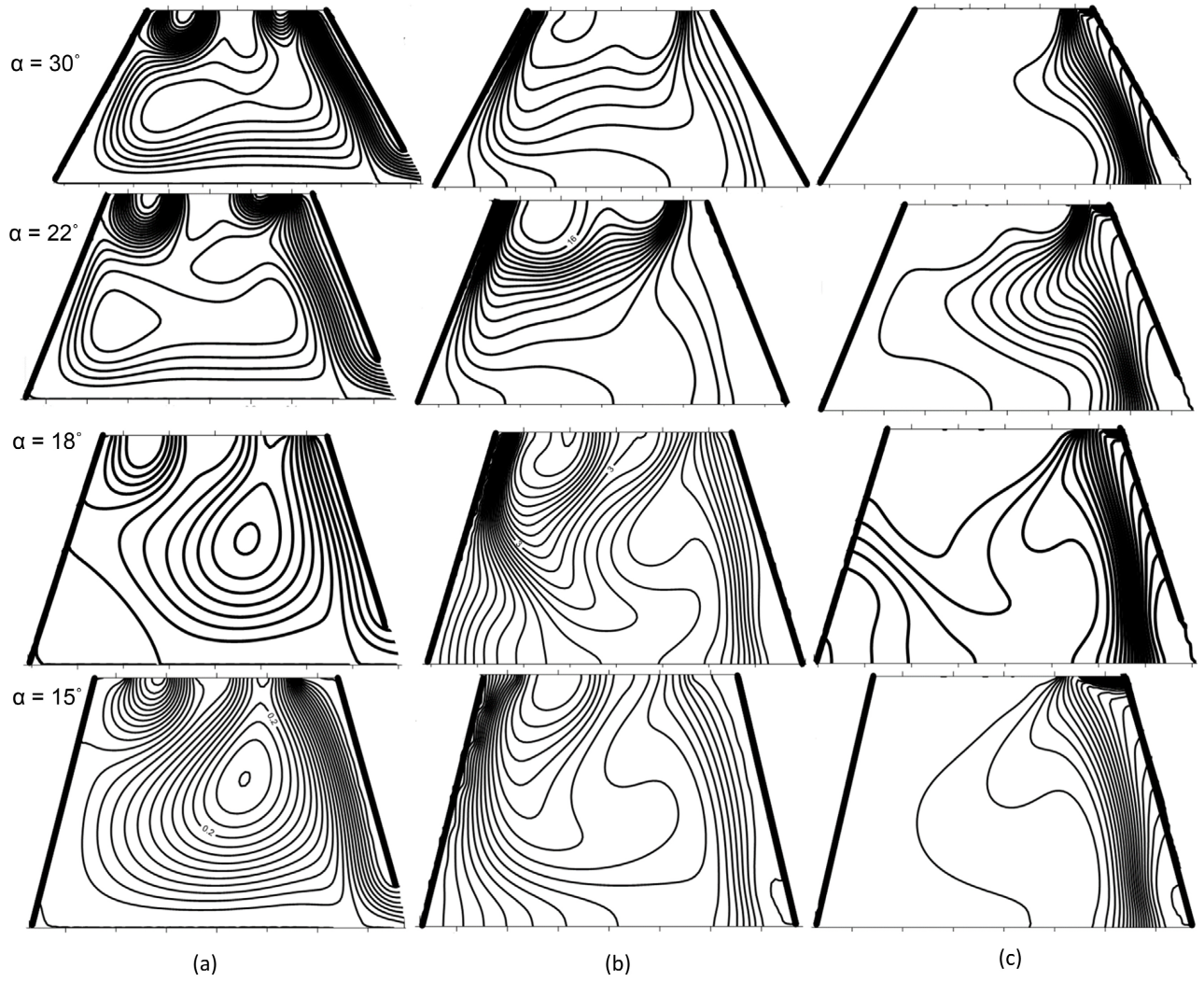

Figure 5. Streamlines (a), isotherms (b) and humidity contours (c) for $R_i = 0.1$ and for different values of the inclination angles.

cold air jet from the inlet port.

7.2. Mixed Convection ($R_i = 1$)

Figure 6 shows the streamlines, the isotherms and the iso-values of moisture, respectively for $R_i = 1$ and for the inclination angle varying from 15˚ to 30˚. For a Richardson number of $R_i = 1$, the flow structure, isotherms and iso-values of moisture are similar to those observed for $R_i = 0.1$. While the open lines of the flow structure take place from the inlet port go along the right sidewall of the cavity toward the outlet port near to the upper part of the same wall, the recirculating cells appear in the lower part of the cavity limited by the left wall, the top wall and the main flow zone. This zone is dominated by natural convection which becomes more and more important when the inclination angle increases. It can be observed in Figure 6(c) that the size of the zone occupied by moisture contours decreases when the inclination angle increases from $\alpha = 15˚$ to $\alpha = 22˚$ in opposite of those of temperature and streamlines. But for $\alpha = 30˚$, it can be

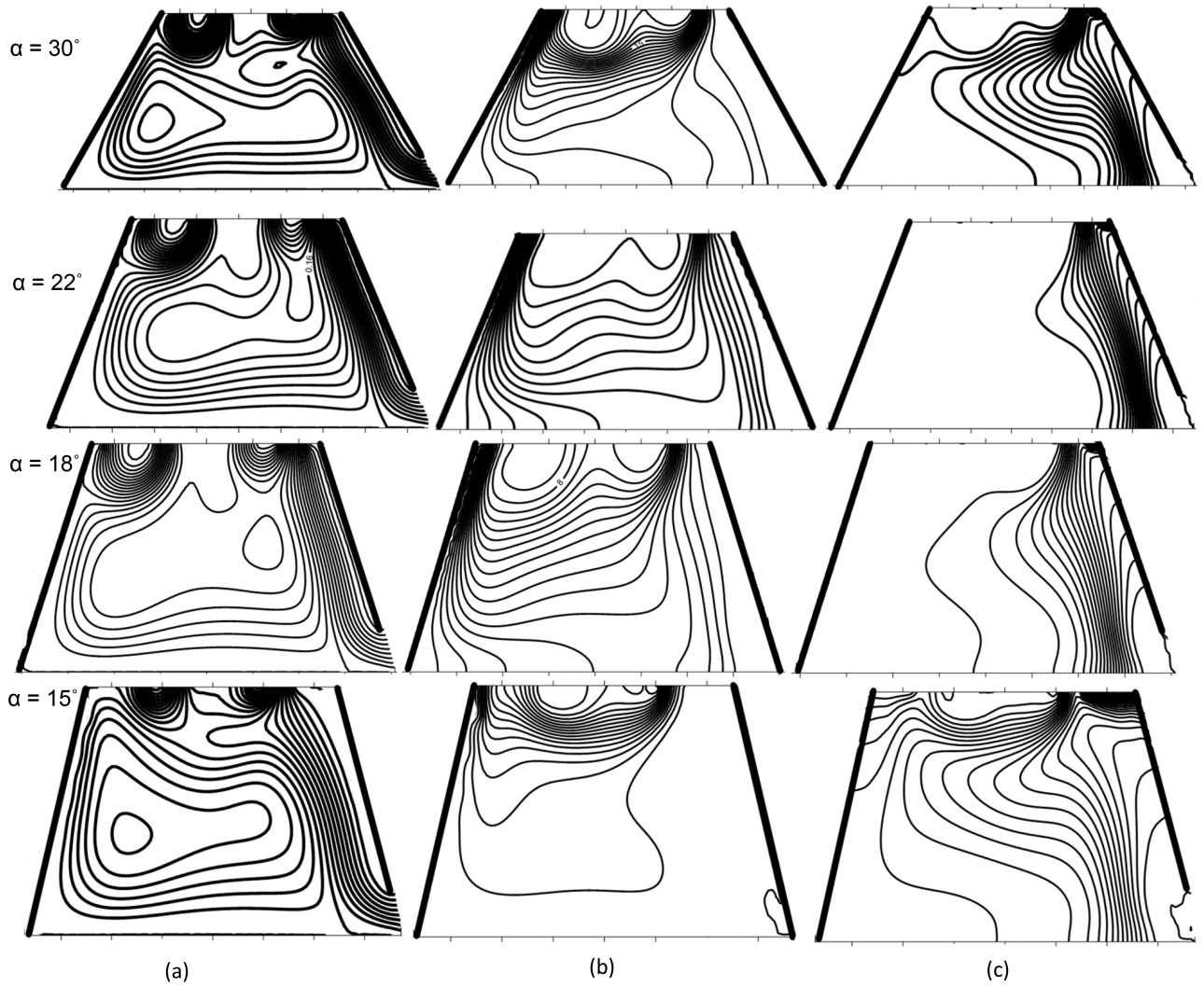

Figure 6. Streamlines (a), isotherms (b) and moisture contours (c) for $R_i = 1$ and for different values of the inclination angles.

noticed an increase of moisture contours and the decreasing of temperature contours due to the cold air resulting from the installation of forced convection.

7.3. Dominance of Natural Convection (R_i = 10; 100)

Figure 7 shows the streamlines, isotherms and moisture contours for $R_i = 10$ and for the inclination angle varying from 15˚ to 30˚. The flow is characterized by open lines going from the inlet to the outlet ports along the right wall which creates a clockwise cell in the cavity for all inclination angle values. Natural convection is becoming less and less important by decreasing the inclination angle. It is shown by recirculation cells of triangular shapes tending to occupy the cavity from the top of the left sidewall passing through the lower left corner and then along the lower horizontal wall. It can be noted the appearance of a secondary vortex in the center of these recirculation cells, but also in the upper right corner of the cavity (Figure 7(a)). When the inclination angle decreases, corresponding to $\alpha = 22^\circ$ and $\alpha = 18^\circ$ (Figure 7(a)), another cell appears in the

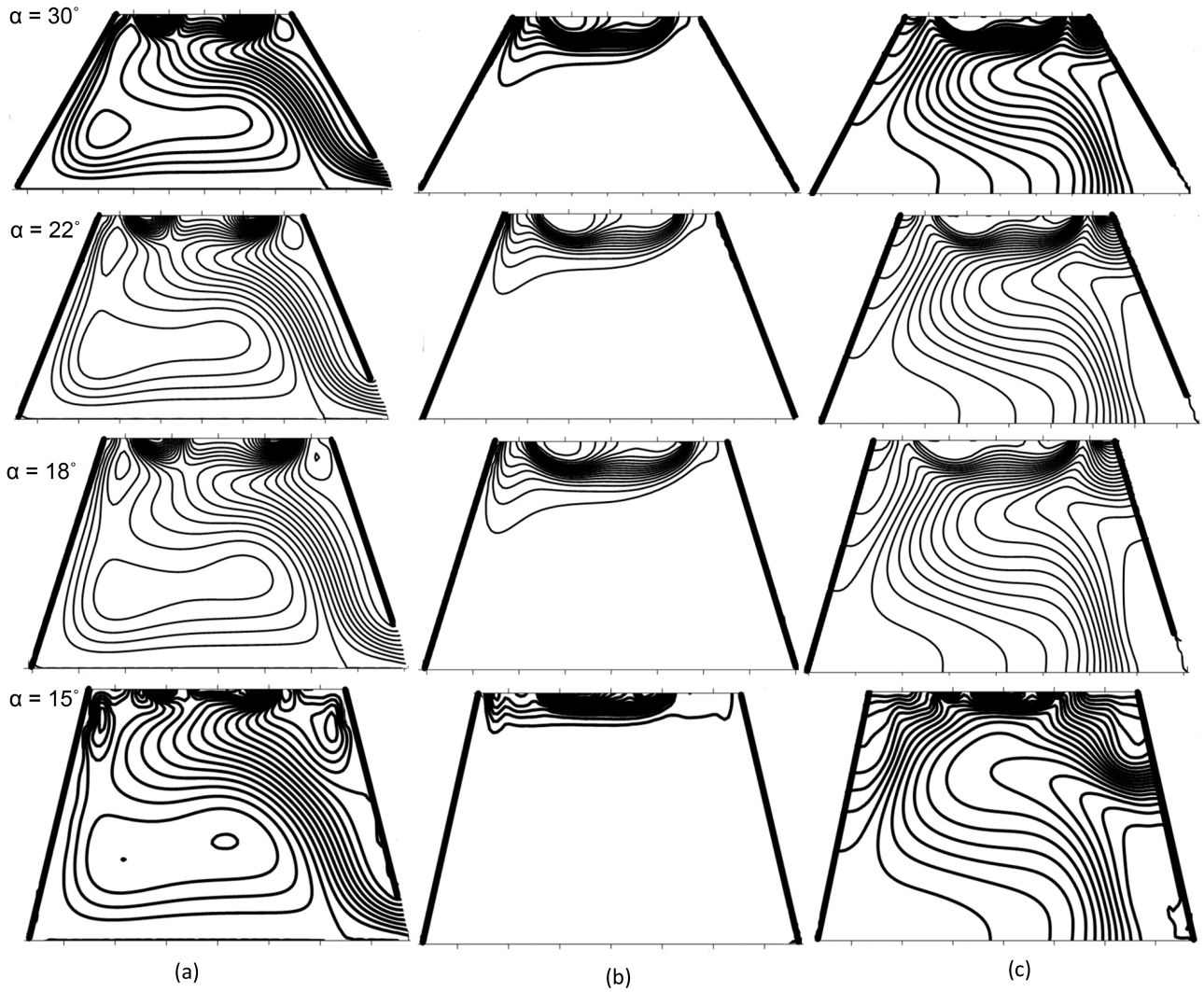

Figure 7. Streamlines (a), isotherms (b) and humidity contours (c) for $R_i = 10$ and for different values of the inclination angles.

upper left corner. The recirculation cells observed for all values of inclination angle can be explained by the buoyancy forces of mass which are more important in the lower zone of the cavity than the vicinity of the top grid (**Figure 7(a)**).

For $\alpha = 15^{\circ}$ (**Figure 7(a)**), the open lines cross the cavity diagonally from the inlet to the outlets. This value of the inclination angle seems to provide a better draft, because promoting the intensification of the open lines. The isotherms are weakly affected with respect to the increasing of the inclination angle (**Figure 7(b)**). They pile up near the heated upper wall with outlets. **Figure 7(c)** shows de moisture contours which take place in the major part of the cavity. The distribution of moisture in the cavity is affected by the rise of the temperature and the intensification of naturel convection transfer in the cavity resulting from the gradient of temperature between the heated grid located at the upper wall and the cold air laden with moisture entering inside the cavity.

In order to confirm the results for natural convection, the Richardson number

is increased to 100. Figure 8 shows the streamlines (a), isotherms (b) and moisture contours (c) for $R_i = 100$ and for different values of the inclination angles. It can be observed that as the inclination decreases, the main flow tending to cross the cavity along the diagonal appears (Figure 8(a)). This main flow becomes intense by reducing the size of the convective cell which is then located in the lower left angle promoting at the same time the shearing effect, which will lead to the formation of a contrarotative cell above the jet (Figure 8(a) for $\alpha = 22^\circ$ and $\alpha = 30^\circ$). The development of the intense recirculating cells just at the entrance of the cavity prevents a free draft of air towards the exits (Figure 8(a) for $\alpha = 30^\circ$ and for $\alpha = 22^\circ$). It can also be noticed that, in the rest of the cavity, low intensity recirculation cells appear. Figure 8(b) and Figure 8(c) illustrate the distribution of temperature and moisture in the cavity for different inclination angle values.

The analysis of these figures shows that the isotherms and moisture contours are tight near the top wall with exits. The moisture contours tend to take place in

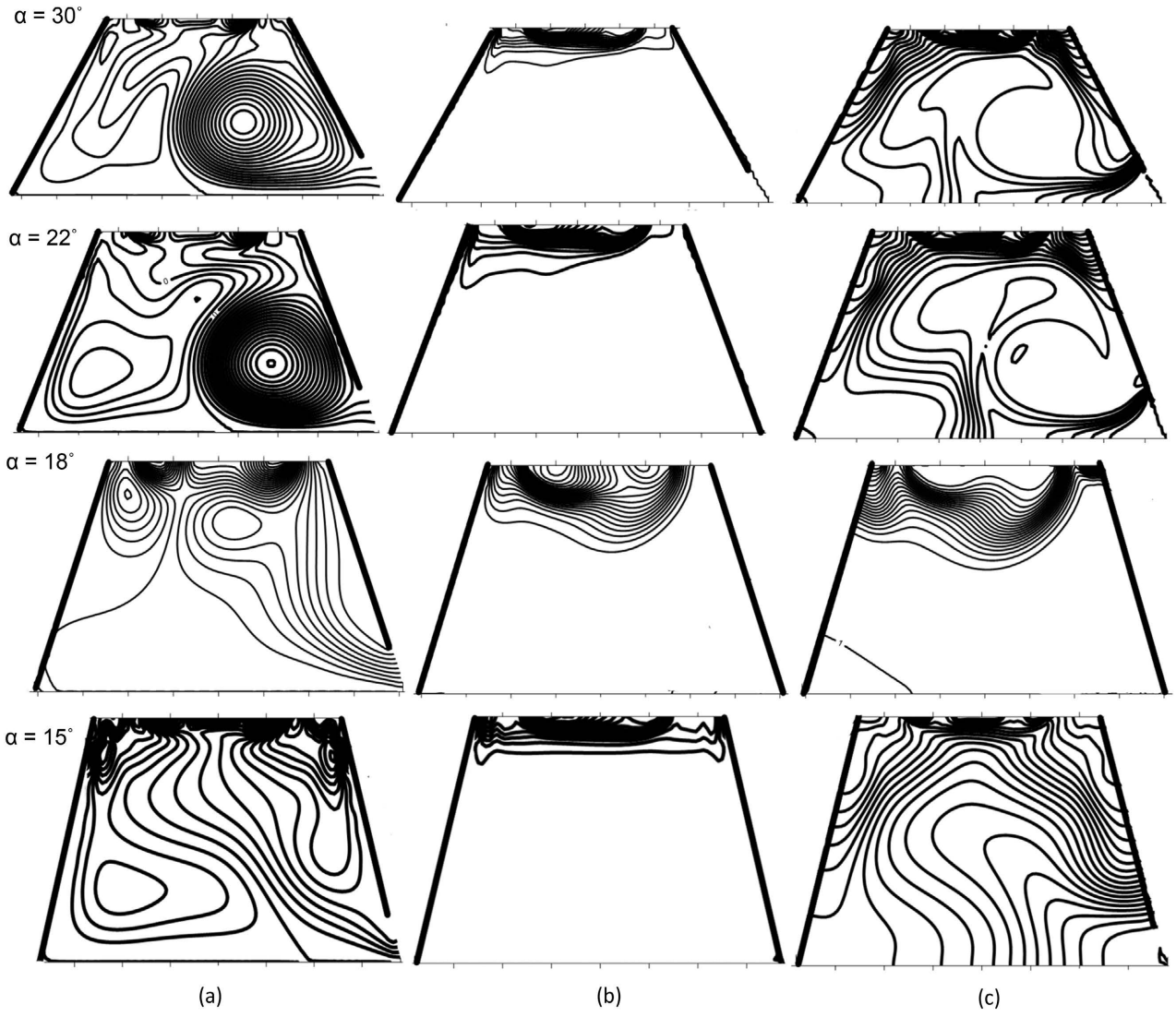

Figure 8. Streamlines (a), isotherms (b) and moisture contours (c) for $R_i = 100$ and for different values of the inclination angles.

all the cavity when the inclination angle increases. They are tighter at the vicinity of the sidewalls than in the middle of the cavity where their distortions are more important due to the recirculation cells of air flow observed in this zone.

8. Conclusions

A numerical study of heat and mass transfer in mixed convection inside a trapezoidal cavity with an inlet and a grid at the upper part is investigated. The analysis focuses on the influence of the inclination angle on the structure of flow, heat and moisture transfers for different Richardson values.

The results show that for a given Richardson number, the variation of the inclination is a control factor of the flow structure, the distribution of temperature and moisture of air in the cavity. For all considered Richardson number, the flow structure is characterized by open lines and recirculation cells denoting the presence of forced convection and naturel convection. For low Richardson number (R_i = 0.1 and R_i = 1), the isotherms are developed in all the cavity while the moisture contours are located near the right sidewall where the forced flow of cold air is more important. When the Richardson number is higher (R_i = 10 and R_i = 100), the isotherms are tight to the heated grid and the moisture contours are developed in all the cavity. For all Richardson number considered, the decrease in the inclination angle leads to the disappearance of closed lines in favor of open lines promoting the draft. For R_i = 1, an optimum air draft corresponds to an inclination angle of the sidewall of ASUTO charcoal stove draft zone is in the vicinity of 22˚ while for R_i = 10 or 100, the optimum inclination angle for air draft is in the vicinity of 15˚. This inclination angle is retained to promote the best air draft into the combustion chamber of the stove when functioning in natural convection.

In the future work, we will couple this primary air draft zone to the cookstove combustion chamber considered as a reactive porous medium, in order to account for the global operation of the cookstove and then move on to the experiment.

Conflicts of Interest

The authors declare no conflicts of interest regarding the publication of this paper.

References

[1] Sedighi, M. and Salarian, H. (2017) A Comprehensive Review of Technical Aspects of Biomass Cookstoves. *Renewable and Sustainable Energy Reviews*, **70**, 656-665. https://doi.org/10.1016/j.rser.2016.11.175

[2] Bryden, M., *et al.* (2005) Design Principals for Wood Burning Cookstoves. Aprovecho Research Center, Cottage Grove.

[3] Kumar, M., Kumar, S. and Tyagi, S.K. (2013) Design, Development and Technological Advancement in the Biomass Cookstoves: A Review. *Renewable and Sustainable Energy Reviews*, **26**, 265-285. https://doi.org/10.1016/j.rser.2013.05.010

[4] MacCarty, N., Still, D. and Ogle, D. (2010) Fuel Use and Emissions Performance of Fifty Cookingstoves in the Laboratory and Related Benchmarks of Performance. *Energy for Sustainable Development*, **14**, 161-171. https://doi.org/10.1016/j.esd.2010.06.002

[5] Baldwin, S.F. (1987) Biomass Stoves: Engineering Design, Development, and Dissemination. Volunteers in Technical Assistance Arlington, VA.

[6] Agenbroad, J., DeFoort, M., Kirkpatrick, A. and Kreutzer, C. (2011) A Simplified Model for Understanding Natural Convection Driven Biomass Cooking Stoves—Part 1: Setup and Baseline Validation. *Energy for Sustainable Development*, **15**, 160-168. https://doi.org/10.1016/j.esd.2011.04.004

[7] Agenbroad, J.N. (2011) A Simplified Model for Understanding Natural Convection Driven Biomass Cooking Stoves—Part 2: With Cook Piece Operation and the Dimensionless form Energy for Sustainable Development, 15, 169-175.

[8] Saadoun, B., Salim, E., Farid, B., Omar, K., Bachir, D. and Abdelkader, F. (2019) Unsteady Mixed Convection in a Cubic Lid-Driven Cavity Partially Heated from the Bottom. *Journal of Advanced Research in Fluid Mechanics and Thermal Sciences*, **57**, 275-287.

[9] Mourabit, M., Rouijaa, H., Semma, E.A. and Alami, M.E. (2014) Etude numérique de l'effet d'inclinaison d'une cavité en forme. de 'T'sur la symétrie de la solution et le transfert de chaleur. *Revue des Energies Renouvelables*, **17**, 519-527.

[10] Kent, E.F. (2009) Numerical Analysis of Laminar Natural Convection in Isosceles Triangular Enclosures. *Proceedings of the Institution of Mechanical Engineers, Part C*, **223**, 1157-1169. https://doi.org/10.1243/09544062JMES1122

[11] Projahn, U., Rieger, H. and Beer, H. (1981) Numerical Analysis of Laminar Natural Convection between Concentric and Eccentric Cylinders. *Numerical Heat Transfer*, **4**, 131-146. https://doi.org/10.1080/01495728108961783

[12] Yalcin, H.G., Baskaya, S. and Sivrioglu, M. (2008) Numerical Analysis of Natural Convection Heat Transfer from Rectangular Shrouded Fin Arrays on a Horizontal Surface. *International Communications in Heat and Mass Transfer*, **35**, 299-311. https://doi.org/10.1016/j.icheatmasstransfer.2007.07.009

[13] Lam, S.W., Gani, R. and Symons, J.G. (1989) Experimental and Numerical Studies of Natural Convection in Trapezoidal Cavities. *Journal of Heat Transfer*, **111**, 372-377. https://doi.org/10.1115/1.3250687

[14] Boussaid, M., Mezenner, A. and Bouhadef, M. (1999) Convection naturelle de chaleur et de masse dans une cavite trapezoidale. *International Journal of Thermal Sciences*, **38**, 363-371. https://doi.org/10.1016/S1290-0729(99)80103-3

[15] Acharya, S. (2000) Natural Convection in Trapezoidal Cavities with Baffles Mounted on the Upper Inclined Surfaces. *The impact score (IS) 2020 of Numerical Heat Transfer; Part A*: *Application*, **37**, 545-565. https://doi.org/10.1080/104077800274082

[16] Fontana, É., da Silva, A., Mariani, V.C. and Marcondes, F. (2010) The Influence of Baffles on the Natural Convection in Trapezoidal Cavities. *Numerical Heat Transfer*, *Part A*: *Applications*, **58**, 125-145. https://doi.org/10.1080/10407782.2010.496673

[17] da Silva, A., Fontana, É., Mariani, V.C. and Marcondes, F. (2012) Numerical Investigation of Several Physical and Geometric Parameters in the Natural Convection into Trapezoidal Cavities. *International Journal of Heat and Mass Transfer*, **55**, 6808-6818. https://doi.org/10.1016/j.ijheatmasstransfer.2012.06.088

[18] Benzema, M., Benkahla, Y.K., Labsi, N., Brunier, E. and Ouyahia, S.-E. (2017) Numerical Mixed Convection Heat Transfer Analysis in a Ventilated Irregular Enclo-

sure Crossed by Cu-Water Nanofluid. *Arabian Journal for Science and Engineering*, **42**, 4575-4586. https://doi.org/10.1007/s13369-017-2563-6

[19] Munshi, M., Mostafa, G., Munsi, A. and Waliullah, M. (2018) Hydrodynamic Mixed Convection in a Lid-Driven Hexagonal Cavity with Corner Heater. *American Journal of Computational Mathematics*, **8**, 245-258. https://doi.org/10.4236/ajcm.2018.83020

[20] Benzema, M., Benkahla, Y.K., Labsi, N., Ouyahia, S.-E. and El Ganaoui, M. (2019) Second Law Analysis of MHD Mixed Convection Heat Transfer in a Vented Irregular Cavity Filled with Ag-MgO/Water Hybrid Nanofluid. *Journal of Thermal Analysis and Calorimetry*, **137**, 1113-1132. https://doi.org/10.1007/s10973-019-08017-x

[21] Gogoi, B. and Baruah, D.C. (2016) Steady State Heat Transfer Modeling of Solid Fuel Biomass Stove: Part 1. *Energy*, **97**, 283-295. https://doi.org/10.1016/j.energy.2015.12.130

[22] Mahmoudi, A.H., Pop, I., Shahi, M. and Talebi, F. (2013) MHD Natural Convection and Entropy Generation in a Trapezoidal Enclosure Using Cu-Water Nanofluid. *Computers & Fluids*, **72**, 46-62. https://doi.org/10.1016/j.compfluid.2012.11.014

[23] Aydin, O. and Yang, W.-J. (2000) Mixed Convection in Cavities with a Locally Heated Lower Wall and Moving Sidewalls. *Numerical Heat Transfer*, *Part A*: *Applications*: *An International Journal of Computation and Methodology*, **37**, 695-710. https://doi.org/10.1080/104077800274037